



OPEN ACCESS

EDITED BY

Spyridon Alexandros Petropoulos,
University of Thessaly, Greece

REVIEWED BY

Ágnes Szepesi,
University of Szeged, Hungary
Yong Liu,
Hunan Academy of Agricultural Sciences
(CAAS), China

*CORRESPONDENCE

Jin Xue

✉ xuejin@hunau.edu.cn

Xiaolan Liao

✉ liaoxl88@126.com

Xiaogang Li

✉ lxgang@hunau.edu.cn

RECEIVED 30 October 2023

ACCEPTED 24 April 2024

PUBLISHED 14 May 2024

CITATION

Zhong S, Guo C, Su L, Jiang H, Wang X-e,
Shi L, Li X, Liao X and Xue J (2024)
Physiological and transcriptomic analyses
provide preliminary insights into the
autotoxicity of *Lilium brownii*.
Front. Plant Sci. 15:1330061.
doi: 10.3389/fpls.2024.1330061

COPYRIGHT

© 2024 Zhong, Guo, Su, Jiang, Wang, Shi, Li,
Liao and Xue. This is an open-access article
distributed under the terms of the [Creative
Commons Attribution License \(CC BY\)](#). The
use, distribution or reproduction in other
forums is permitted, provided the original
author(s) and the copyright owner(s) are
credited and that the original publication in
this journal is cited, in accordance with
accepted academic practice. No use,
distribution or reproduction is permitted
which does not comply with these terms.

Physiological and transcriptomic analyses provide preliminary insights into the autotoxicity of *Lilium brownii*

Shumin Zhong, Chuibao Guo, Lu Su, Han Jiang, Xue-er Wang,
Li Shi, Xiaogang Li*, Xiaolan Liao* and Jin Xue*

Hunan Provincial Key Laboratory for Biology and Control of Plant Diseases and Insect Pests, College of Plant Protection, Hunan Agricultural University, Changsha, China

Lilium brownii F. E. Brown ex Mieliez var. *viridulum* Baker (Longya lily) is a variety of *Lilium brownii* F.E. Br. ex Mieliez. We used HS-SPME and GC-MS to screen the tissues of *L. brownii* roots, stems, bulbs, and leaves and obtained 2,4-DTBP as an autotoxic substance for subsequent analysis. 2,4-DTBP was highly autotoxic in some treatment groups. Based on changes in physiological indicators, we carried out transcriptomic analysis to investigate the mechanisms of autotoxicity of substances on *L. brownii* and obtained 188,505 Unigenes. GO and KEGG enrichment analyses showed that *L. brownii* responded differently to different concentrations and treatment times of 2,4-DTBP. We observed significant changes in genes associated with ROS, phytohormones, and MAPK signaling cascades. 2,4-DTBP affects chloroplasts, the integrity of the respiratory electron transport chain, and ribosomes, causing *L. brownii* autotoxicity. Our findings provide a practical genomic resource for future research on *L. brownii* autotoxicity and evidence for the mechanism of action of autotoxic substances.

KEYWORDS

Lilium brownii, phenolic, autotoxicity, transcriptome, reactive oxygen species (ROS), phytohormone

1 Introduction

Lilium brownii is a perennial bulbous herb from the family Liliaceae that is used as a traditional Chinese herb. Its bulbs are rich in sugars, proteins, minerals, alkaloids, steroidal saponins, and other active ingredients, making it a popular natural health product that combines medicine and food. *L. brownii* is an important cash crop in Shao yang, Hunan Province, with economic benefits that are three to ten times greater than those of other

crops. The *L. brownii* was designated as a Geographical Indication product in 2009, but there were severe Continuous Cropping Obstacles (CCO) in its production. For successive cultivations of *L. brownii*, soil sampling revealed significant acidification, along with severe outbreaks of pests and diseases, for which chemical control was inefficient.

Problems related to CCO have been reported in other crops (Zeng et al., 2020; Huang et al., 2021; Ku et al., 2022; Wang et al., 2022; Yan et al., 2022). Plant autotoxicity is thought to be a key contributing factor to the development of CCO. Autotoxicity affects the soil environment, microorganisms, and the crop itself by inhibiting the normal physiological functioning of chronically affected crops. Autotoxicity also causes soil acidification, nutrient imbalances, reduced enzyme activity, and an increase in pathogenic microorganisms (Gao et al., 2019; Chen et al., 2020a; Li et al., 2021). These effects have resulted in significant reductions in crop yields, increased rates of plant diseases, and the need to frequently change the land on which crops are grown, causing significant problems for agricultural production.

Secondary metabolite production is associated with plant adaptation to the environment in response to external stressors (Li et al., 2019b; Wu et al., 2020; Chen et al., 2020b; Yu et al., 2021). For example, phycocyanin and lignin are secondary metabolites that can act as biochemical barriers against invading pathogens (Ahuja et al., 2012; Gallego-Giraldo et al., 2018). Secondary metabolites are also involved in signaling plant disease resistance responses (Erb and Kliebenstein, 2020) and suppressing Herbivore-Induced defense signaling (Li et al., 2019a). Autotoxicity occurs when secondary metabolites produced by the decomposition of leachate and residues from plant roots, stems, and leaves, or chemicals secreted by a plant inhibit the growth of the plant's roots, decrease its activity, and inhibit the growth of crops of the same species or the following crop.

The most commonly reported autotoxic substances are phenols and terpenoids, such as benzoic acid (Wu et al., 2015; Xiang et al., 2022), ferulic acid (Chi et al., 2013), p-hydroxybenzoic acid (Wu et al., 2021), and saponins. Autotoxic substances primarily affect the plant cell membrane, chloroplasts, mitochondria, and other cell structures, causing vesicle, cell membrane, and organelle destruction and affecting cell membrane permeability. Autotoxic substances influence plant physiological processes such as hormone homeostasis, oxidative stress response, cellular respiration, and photosynthesis (Kim et al., 2019; Yang et al., 2020; Zhang et al., 2020; Adamakis et al., 2021).

Few studies have investigated autotoxic substances in *L. brownii*. In this study, we isolated and identified the autotoxic substances that causes Continuous Cropping Obstacles from the tissues of *L. brownii*. We analyzed the activity of autotoxic substances and their effects on the physiological biochemistry of *L. brownii*. We used transcriptome sequencing to investigate the molecular mechanisms of autotoxic substance-induced stress in *L. brownii*. Our findings provide a theoretical foundation for

further research into the autotoxic effects of *L. brownii* and aid in managing its Continuous Cropping Obstacles.

2 Materials and methods

2.1 Collection, separation, identification, and screening of autotoxic substances

2.1.1 Collection of *L. brownii* tissue

Samples of fresh, healthy Longya lilies were collected from plants grown at the plant protection base after one-year cultivation at Hunan Agricultural University (28°10'44"N 113°04'29"), Hunan Province, China. The roots, bulbs, stems, and leaves were cleaned and dried at 45°C, then ground and stored at 4°C in the refrigerator for analysis.

Tissue culture plants of *L. brownii* were propagated in our laboratory.

2.1.2 Isolation and identification of autotoxic substances and screening

Headspace solid-phase microextraction was used to isolate autotoxic substances from *L. brownii* samples. The headspace vial was preheated with 0.2 g of ground *L. brownii* for 40 min at 80°C, samples were then extracted for 40 min at 80°C followed by desorption for 5 min.

An GCMS-QP2010 system (Shimadzu, Japan) was used to identify the autotoxic substances isolated from *L. brownii*. The temperature of the injector and ion source was 240°C and 200 °C, respectively. The ionization was carried out in the electron impact (EI) mode at 70 eV. The capillary column was 30.0m length, 0.25 mm i.d., and 0.25 μm film thickness. An initial column temperature was 50°C, retained 4 min, then increased to 200°C at a rate of 6°C/min and held for 10 min, and finally increased to 240°C at the rate of 8°C/min and held for 15 min. Helium was used as a carrier gas at a constant flow of 1.0 mL/min. The MS data were acquired in full scan mode from m/z 45~500 with an acquisition frequency of 2.5 scans per second, according to the method of Deng et al (Deng et al., 2004).

Results were compared and analyzed in the NIST database.

2.2 Bioassay of 2,4-DTBP treatment on *Allium ascalonicum*

Lilium brownii is a perennial plant with a long annual growth cycle that makes observation difficult in the early stages of growth, *Allium ascalonicum*, was selected for the test seed.

Using the GC-MS results, 2,4-DTBP solutions were prepared at concentrations of 0 (CK), 0.05, 0.1, 0.2, 0.4 and 0.8 g/L. 5 mL of each concentration was added to Petri dishes lined with filter paper. Healthy, uniform-sized *Allium ascalonicum* seeds were soaked at 50°C for 30 min, then left to cool naturally in a bottle containing 50°

C water for 2 h. The seeds were then soaked in 5% sodium hypochlorite for 5 min, rinsed three times with sterile water and dried. The *A. ascalonicum* seeds were then evenly distributed in the Petri dishes and incubated at 25°C for 12 h in an illuminating incubator. The germination rate was recorded after 4 d. Root length and stem length were measured after 5 d. Twenty seeds per treatment were used, with three replicates per treatment, according to the method of Wang et al (Wang et al., 2018).

L. brownii tissue culture plants were treated with 0 (CK), 0.2, and 0.8 g/L of 2,4-DTBP to observe the effects of autotoxic substances.

Data are expressed as means \pm standard errors. Differences were analyzed using one-way analysis of variance (ANOVA) and least significant difference (LSD) in SPSS 22.0 for Windows (SPSS, Inc., Chicago, IL, USA). $P < 0.05$ was considered significant.

2.3 Physiological and biochemical measurements of *Lilium brownii* after 2,4-DTBP treatment

L. brownii bulbs were placed in a hydroculture solution containing 0 (CK), 0.05, 0.2, and 0.8 g/L of 2,4-DTBP and sampled at 9 h, 12 h, 24 h, 72 h, and 120 h, and the content of superoxide dismutase (SOD), peroxidase (POD) activity, and malondialdehyde (MDA) was measured. Superoxide dismutase activity was determined using the nitrogen blue tetrazolium (NBT) method, peroxidase (POD) activity using the guaiacol method, and malondialdehyde (MDA) content using the thiobarbituric acid method.

2.4 Transcriptome sequencing of *Lilium brownii* under 2,4-DTBP stress

2.4.1 Plant sample preparation

We used 0 (CK), 0.05, and 0.8 g/L 2,4-DTBP solutions for the *L. brownii* hydroculture. *L. brownii* root samples were collected at 9h, 24h, and 120h, washed with sterile water, blotted dry with sterile filter paper, immediately frozen in liquid nitrogen, and stored at -80°C in the refrigerator.

2.4.2 RNA extraction, library construction, and sequencing

Total RNA was extracted using a Trizol reagent kit (Invitrogen, Carlsbad, CA, USA) according to the manufacturer's protocol. RNA quality was assessed on an Agilent 2100 Bioanalyzer (Agilent Technologies, Palo Alto, CA, USA) and checked using RNase-free agarose gel electrophoresis. Prokaryotic mRNA was enriched by removing rRNA by Ribo-Zero™ Magnetic Kit (Epicentre, Madison, WI, USA). The ligation products were size selected by agarose gel electrophoresis, PCR amplified, and sequenced using Illumina novaseq 6000 by Gene Denovo Biotechnology Co. (Guangzhou, China).

2.4.3 Unigene function annotation

DESeq2 software was used to analyze RNA differential expression between two different groups (and by edgeR between two samples). Genes with a false discovery rate (FDR) below 0.05 and an absolute fold change ≥ 2 were considered differentially expressed. DEGs were analyzed using gene ontology (GO) and Kyoto Encyclopedia of Genes and Genomes (KEGG) enrichment.

2.5 Validation of expression profiles by qPCR

To verify the reliability of the RNA-seq results, nine genes with differential expression in each period were randomly selected for qPCR validation. The RNA extracted earlier was reverse transcribed using an Evo M-MLV RT Premix for qPCR (Accurate Biotechnology [Hunan]). We designed qPCR primers for the selected genes using Primer 3.0 (<https://bioinfo.ut.ee/primer3-0.4.0/>), with EIF and BHLH serving as internal reference genes. For the qPCR experiments we used the SYBR® Green Premix Pro Taq HS qPCR Kit (Accurate Biotechnology [Hunan]) in the Bio-Rad CFX96 system. Relative expression levels were calculated using $2^{-\Delta\Delta Ct}$ and normalized by the average of the two internal reference gene expressions. Each treatment had three biological replicates.

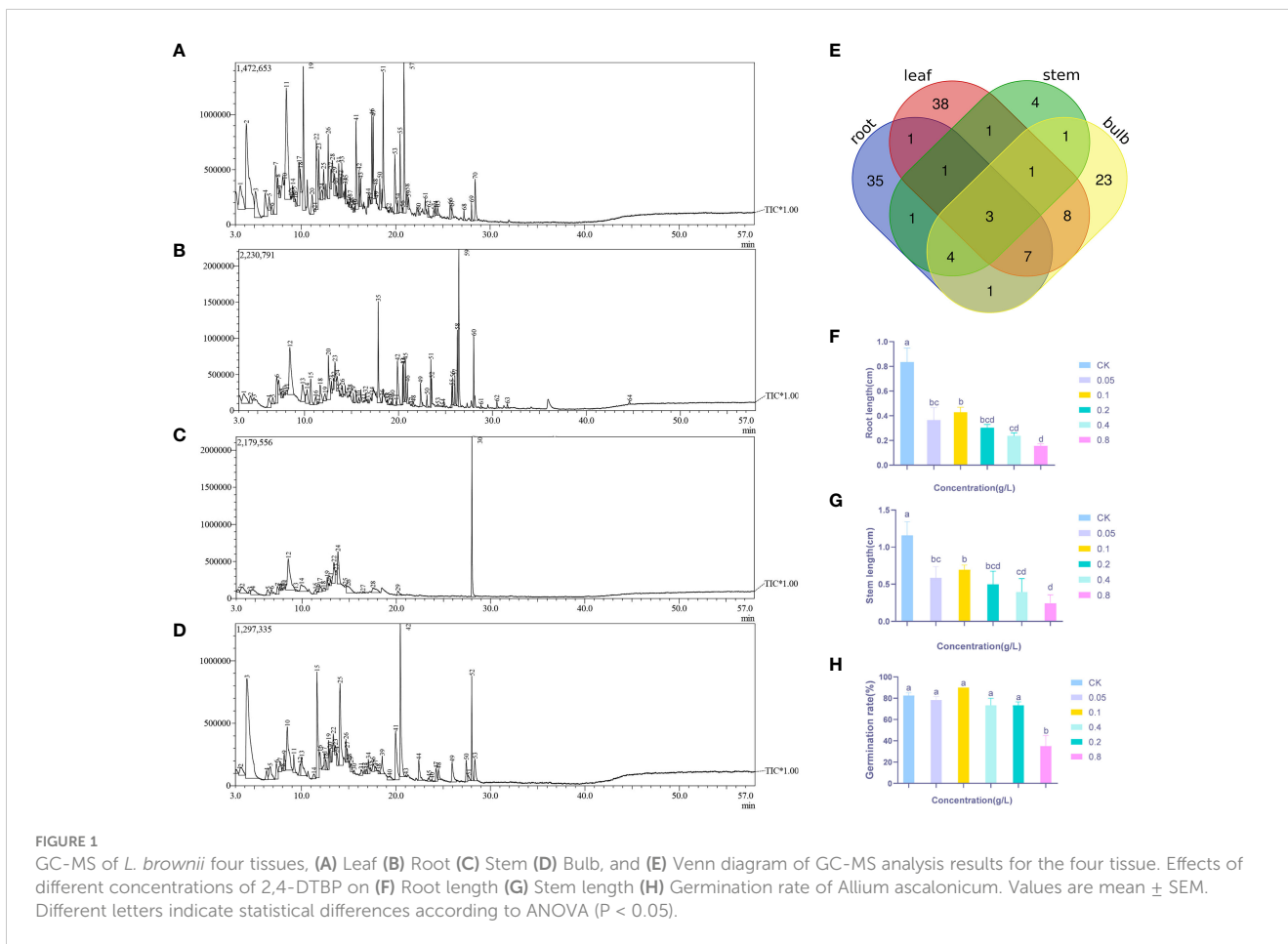
2.6 Tissue culture seedlings of *L. brownii* reprocessing with 2,4-DTBP

To confirm the impact of 2,4-DTBP on the oxidative phosphorylation and hormones of *L. brownii* as the transcriptome described, we treated tissue culture seedlings of *L. brownii* by the same method as the treatment did for the transcriptome analysis. Tissue culture seedlings with consistent growth of *L. brownii* were sampled after treatment with 0, 0.2 and 0.8 g/L of 2,4-DTBP for 0, 9 and 120 hours, respectively. Seedlings were planted in rooting medium containing 2.3 g/L MS, 0.1 mg/L NAA, 7 g/L agar and 25 g/L sucrose. The medium was supplemented with 2,4-DTBP mother liquor to a final concentration of 0, 0.2, and 0.8 g/L. Each treatment had three replicates. DEGs which are pertinent with oxidative phosphorylation and hormones pathways were chosen for validation. The succinate dehydrogenase (SDH) was extracted and the activity was determined by following the procedure outlined in the SDH test kit (Solarbio, BC0950).

3 Results

3.1 Isolation and identification of autotoxic substances and screening

Headspace solid-phase microextraction followed by GC-MS (Figures 1A–D) was performed on the roots, bulbs, stems, and leaves of *Lilium brownii*. There were 64 peaks with more than 80%



similarity. The compounds identified from the four tissues were categorized and showed a high degree of variability between the tissues (Supplementary Table S1). The roots, bulbs, and leaves contained the most compounds with 53, 48, and 60 compounds, respectively (Table 1). Only 16 compounds were isolated from the stems. The roots contained primarily phenol and alcohol compounds, while the leaves and bulbs contained mainly

aldehydes. No ester compounds were identified in the stems. The roots, stems leaves, and bulbs contained heptadecane, 2,4-di-tert-butylphenol, and 2,4-dimethyl benzaldehyde, and all expect bulbs contained 4-methyl dodecane. The bulbs, roots, and stems contained n-hexadecane, 2-ethyl hexanol, (2-methyl propyl) nonane, and hexanal, while the leaves, bulbs, and stems contained n-tetradecane. The three most diverse compounds shared by bulbs,

TABLE 1 Results of GC-MS analysis of *L. brownii*.

substance	tissues			
	roots	stems	bulbs	leaves
phenols	11	1	1	1
aldehydes	4	2	12	14
esters	5	/	5	7
alcohols	16	2	7	4
organic acids	5	1	6	4
others	12	10	17	30
total	53	16	48	60

leaves, and roots were decanal, heptanoic acid, n-dodecane, D-(-)-pantolactone, octanoic acid, trans-2-noninal, and hexanoic acid.

The majority of autotoxic substances were phenolic, ester, saponin, and other compounds. Screening 2,4-DTBP, an autotoxic substance, was performed by combining the number of occurrences of each compound in each tissue of the plant in the Venn diagram (Figure 1E). The effect of 2,4-DTBP on *Allium ascalonicum* (Liliaceae crop) root length, stem length, and seed germination rate was determined separately (Figures 1F–H).

3.2 Effect of 2,4-DTBP on the enzymatic activity of *Lilium brownii*

POD and SOD activities in CK-treated *L. brownii* increased significantly after 24 h (Figures 2B, C). The high level of POD activity remained constant at 72 h, whereas the MDA content was elevated between 12–24 h but then leveled off between 24–72 h. POD and SOD activities were inhibited by 2,4-DTBP at concentrations of 0.05 g/L and 0.2 g/L compared to CK. At 0.2 g/L 2,4-DTBP, POD and SOD activities increased between 9h and 24 h reaching a peak at 120 h. In contrast, the MDA content remained the same. Additionally, the increase in POD activity did not inhibit membrane lipid peroxidation. Under 0.8 g/L 2,4-DTBP treatment conditions, POD and SOD enzyme activity remained at the same level as CK. In contrast, MDA content increased significantly compared to CK at the beginning of 12 h and remained at the same level as CK in the subsequent process. High concentrations of 2,4-DTBP treatment caused irreversible damage to the cell membrane structure of *L. brownii*, and changes in antioxidant enzyme activity could not eliminate the stressing effects caused by autotoxic substances.

The MDA content increased with an increase in 2,4-DTBP concentration (Figure 2A), reaching a peak at 24 h. Treatment with a high concentration of 2,4-DTBP accelerated the onset of lipid peroxidation in *L. brownii*. At 12 h, the MDA content in the treatment group increased with the concentration of 2,4-DTBP. The MDA content in all treatment groups returned to relatively low levels at 120 h but was still significantly higher than CK. To investigate the effect of 2,4-DTBP on *L. brownii* under different conditions, we treated roots with CK, 0.05 g/L, and 0.8 g/L 2,4-

DTBP for 9h, 24h, and 120h, and collected samples for transcriptome sequencing.

3.3 Transcriptome analysis of *Lilium brownii*

The 27 samples sequenced generated raw data ranging from 37937896 to 63057410 Unigenes, with 99% clean reads and a Q20 greater than 98% (Supplementary Table S2). The clean reads were assembled using Trinity software 2.1.1, and a total of 188505 Unigenes were obtained with an average length of 807bp, an N50 of 1356bp, a maximum splicing length of 17880bp, and a minimum of 201bp. There were 67437 (35.77%), 51917 (27.54%), 83,329 (44.21%), and 60056 (31.86%) similar Unigene sequences annotated in KEGG, KOG, Nr, and Swiss-Prot, respectively. 40215 Unigenes were simultaneously annotated by four major databases, accounting for 21.33% of the total Unigenes (Figure 3A).

We used analysis of variance to screen significantly different genes with an FDR <0.05 and $|\log_2FC|>1$. Different pairs of groups were compared and the up- and downregulated genes were counted separately (Figure 3B). The number of differential genes varied among the different groups. The control and high-concentration treatment groups had the highest number of differential genes at 120h, with 678 upregulated and 453 downregulated. Enrichment analysis was performed after classification of differential genes using volcano and Wayne plots. KEGG pathway and GO annotations with an FDR < 0.05 were selected for discussion. QPCR was used to investigate the relative expression levels of nine randomly selected differential genes to validate the RNA sequencing results (Figure 3C).

3.4 DEG analysis of the effects 2,4-DTBP concentration gradient on *L. brownii*

Groups treated with higher concentrations of 2,4-DTBP had more active gene expression differences, with a higher number of differential genes at 9h, 24h, and 120h than those treated with lower concentrations of 2,4-DTBP (Figure 4A). There were only four genes with significant difference in gene expression after 9 h of treatment with a low concentration of 2,4-DTBP compared to the

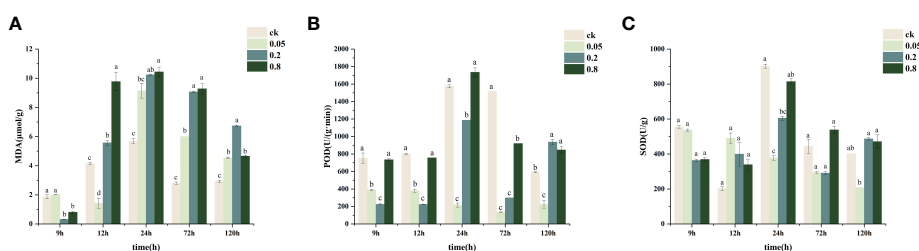
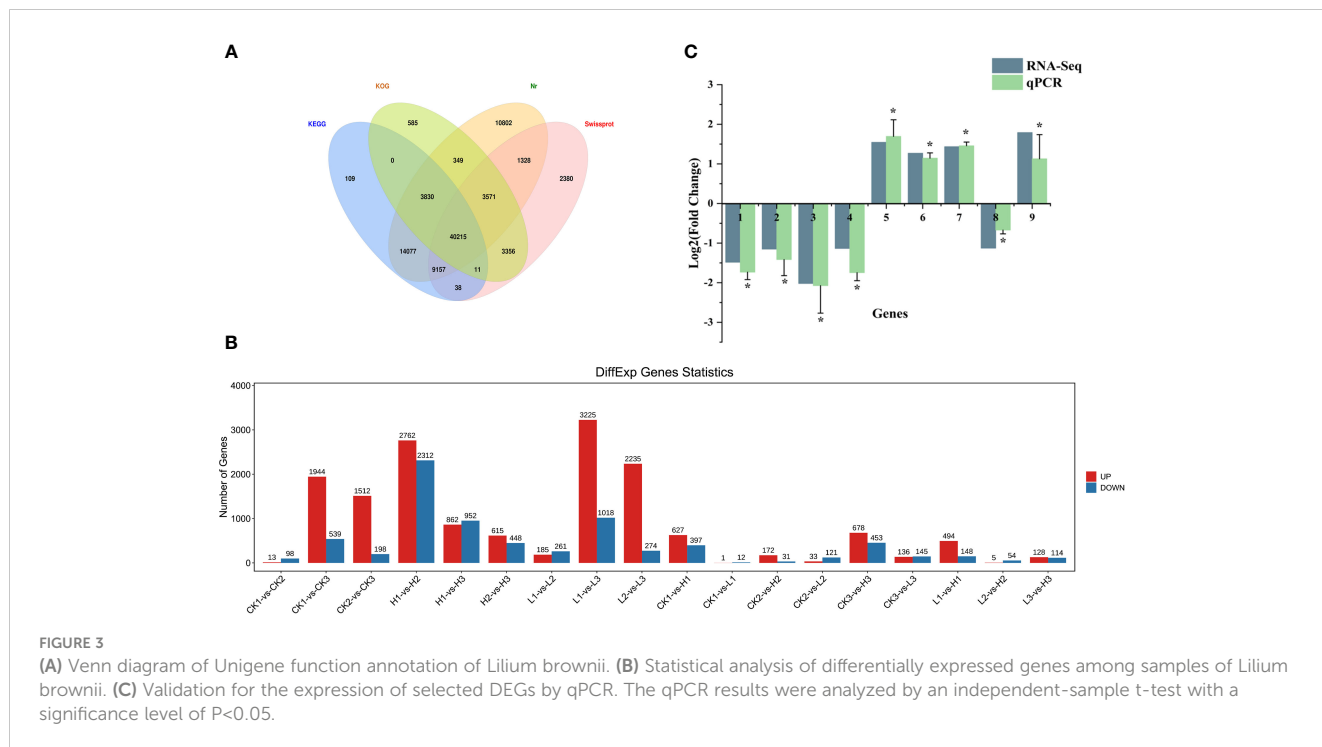


FIGURE 2

Changes in physiological indices of hydroponically grown *Lilium brownii* from 9h to 120h. (A) MDA content (B) Peroxidase activity (C) Superoxide dismutase activity Values are mean + SEM. All experiments were repeated at least three times with similar results.



control. However, after 24 h a significant change in the number of differential genes was observed.

While the high concentration treatment and control groups shared a similar number of differential genes at 9h and 120h, less than 20% were identical (Figure 4B). The specific differential genes present in each of the three time periods were analyzed separately for enrichment analysis (Figures 5A–C). Genes identified at 9h were mainly hormone signaling and ribosome-related genes. GO analysis revealed that the associated differential genes were primarily related to cell wall formation and response to external influences. After 24h, differential genes were mainly associated with mitochondrial membranes and cellular respiration, and at 120h they were mostly associated with cell structure (Figures 5D–F).

Overall, there was an increase in the number of specific differential genes in the low concentration 2,4-DTBP treatment group at 9h, 24h, and 120h compared to the control group. However, within the treatment group there were fewer differential genes at 9h compared to 24h and 120h. KEGG analysis revealed that 24h-specific differential genes were enriched in the Oxidative phosphorylation (Ko00190) and Ribosome (Ko03010) pathways, and at 120h differential genes were primarily enriched in the Ribosome (Ko03010) pathway (Figures 6A, B).

A stress response was observed in *L. brownii* after 9 h treatment with high concentrations of 2,4-DTBP. Auxin, gibberellin, ethylene, and brassinosteroid-related genes in the hormone signal transduction pathway (Ko04075) were significantly downregulated, while abscisic acid, jasmonic acid, and salicylic acid-related genes were significantly upregulated (Figure 6C). After 24 h, annotations related to

respiration, mitochondrial membrane, and electron transport were enriched in both treatment groups compared to CK. However, oxidative phosphorylation-related mitochondrial complexes, cell wall, and endoplasmic reticulum-related genes were differentially expressed in the high-concentration treatment group but not in the low-concentration treatment group.

After 9h, oxidative phosphorylation-related genes were upregulated in the high-concentration treatment group (Figure 6D), but the level of upregulation varied by gene. Furthermore, the 9h annotated transcripts of genes for NADPH dehydrogenase, cytochrome C oxidase, and cytochrome C reductase were significantly more upregulated than for ATPase but not Unigene 0076202 (Figures 6E, F).

3.5 DEG analysis of the effects of 2,4-DTBP treatment time on *L. brownii*

After 24h, the number of differential genes specific to the high-concentration treatment group were several-fold higher than in the low-concentration treatment group and CK, and differentially expressed genes were mainly enriched in primary and secondary metabolic pathways and photosynthesis (Figure 7A). GO enrichment analysis identified 77 biological process annotations that were significantly enriched in response to 2,4-DTBP treatment (Supplementary Table S3). These were mainly related to the photosynthetic membrane (GO:0034357), cell wall (GO:0005618), cytoplasm (GO:0005737), and other structures in the cell membrane (GO:0016020), all of which are associated with

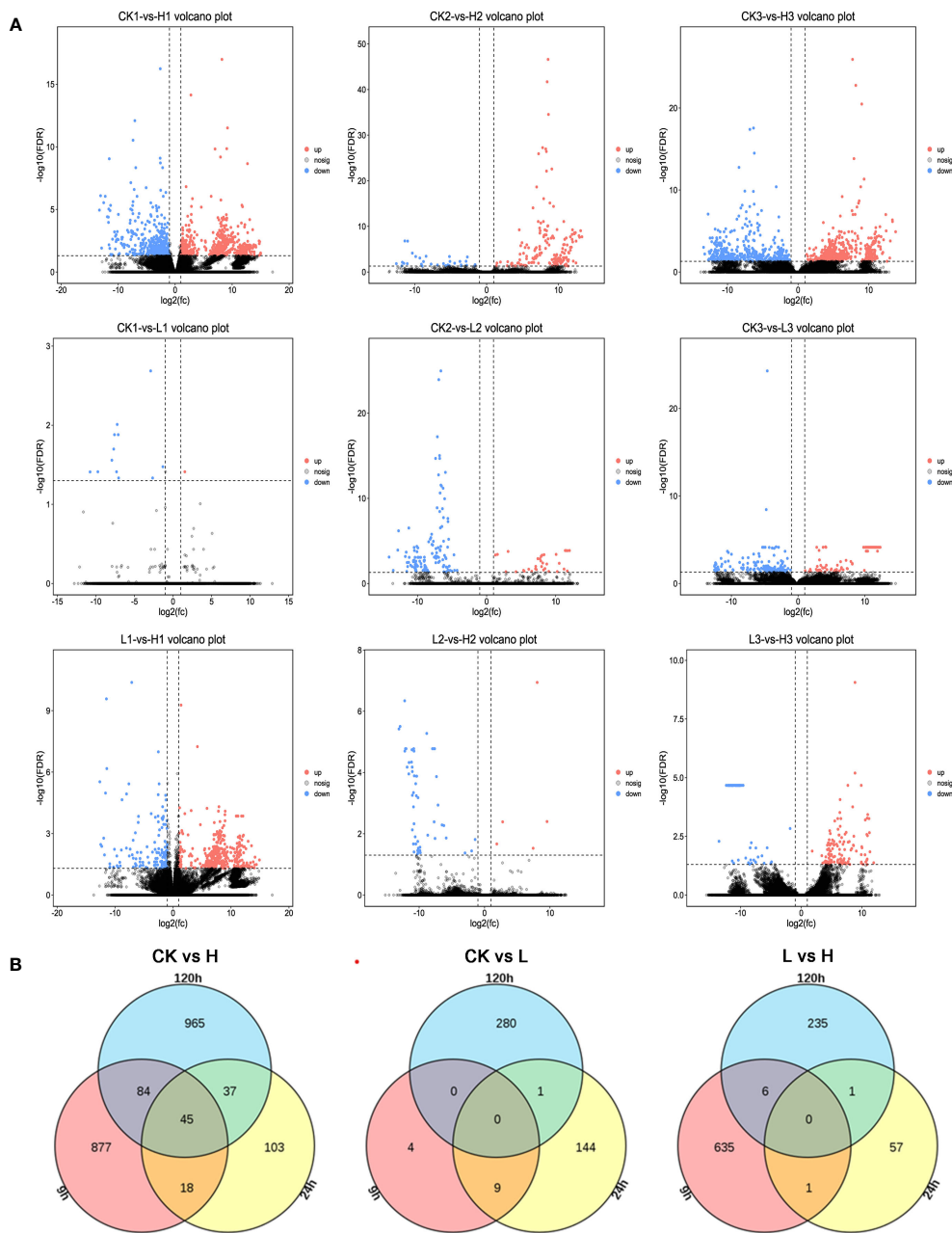


FIGURE 4 (A) Comparison of volcano plots with different concentrations at the same time. The number of DEGs in each tissue is presented and based on the significance shown in the volcano plots. The vertical dash lines in the volcano plots depict the two-fold differential expression cut-off (axis expressed as log₂ values) and the horizontal dash lines shows the -log₁₀(P-value). Dots in red (group₂ up-regulated relative to group₁) and blue (down-regulated) indicate differences in gene expression (FDR < 0.05), while black dots show no differences. (B) Comparison of different treatment groups, Venn diagram of DEGs between various periods.

oxidoreductase activity (GO:0016491). Under low concentration 2,4-DTBP treatment conditions, only the oxidative phosphorylation (Ko00190) and ribosome (Ko03010) pathways were significantly enriched (Figure 7D), with the differential genes primarily involved in processes relating to cellular respiration, including the electron transport chain.

After 120h, the differential genes in CK were associated with cell structure (Figure 7G). Low-concentration treatment resulted in differential genes enriched in ribosomes (Ko03010) and MAPK signaling pathway-plant (Ko04016) (Figure 7E) which are involved in RNA modification (GO:0009451) and ribonucleoprotein complex biogenesis (GO:0022613) processes. High-concentration

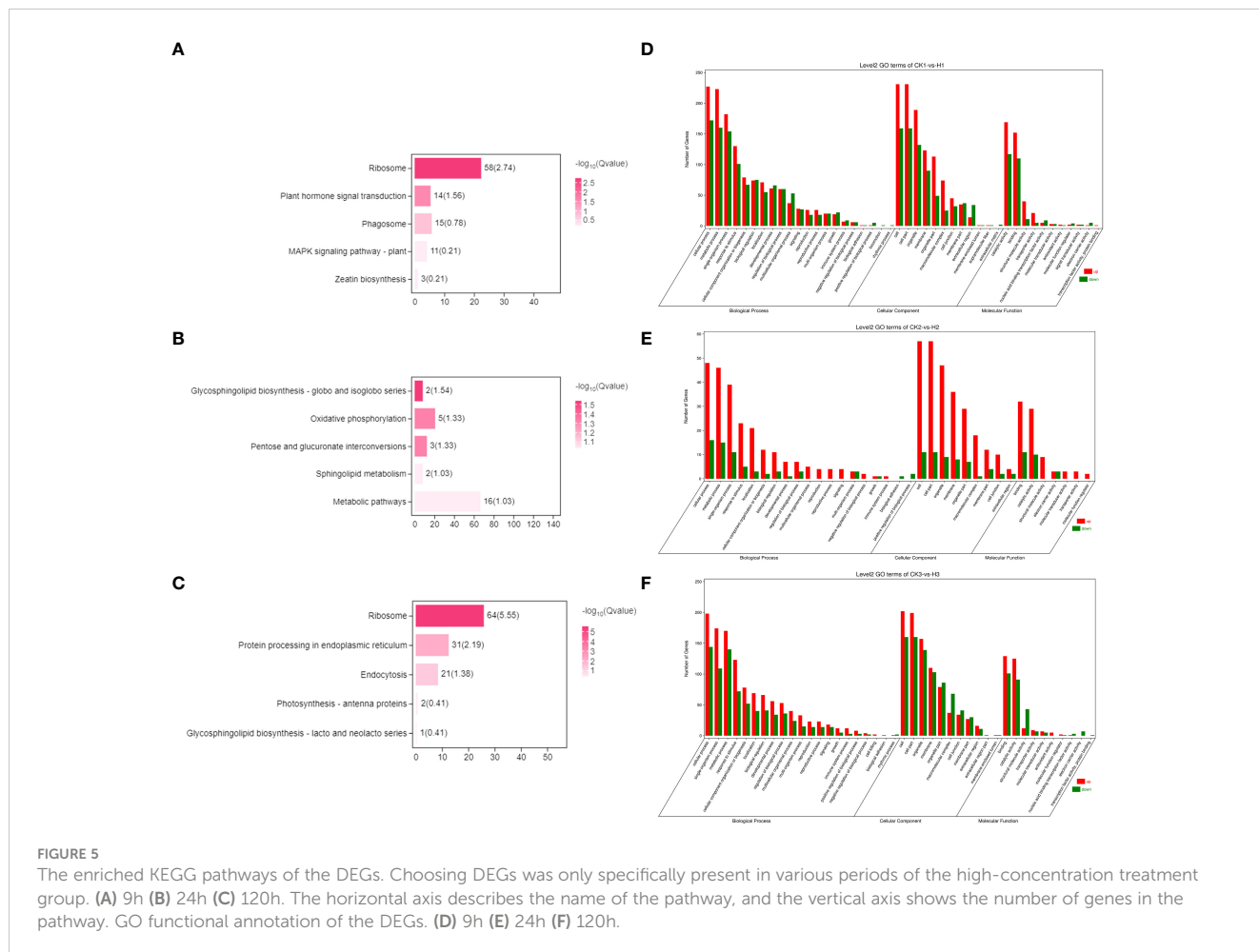


FIGURE 5

The enriched KEGG pathways of the DEGs. Choosing DEGs was only specifically present in various periods of the high-concentration treatment group. (A) 9h (B) 24h (C) 120h. The horizontal axis describes the name of the pathway, and the vertical axis shows the number of genes in the pathway. GO functional annotation of the DEGs. (D) 9h (E) 24h (F) 120h.

treatment for 120h enriched more secondary metabolic pathways than 24h treatment (Figure 7B).

Compared to CK, significantly fewer genes were upregulated in the high-concentration treatment group between 9h and 120h (Figures 7C, 8A). In contrast, gene expression trends were similar between the low-concentration treatment group and CK across all treatment periods. However, the low-concentration treatment group showed a more significant degree of change in gene expression and a greater number of differential genes compared to the high-concentration treatment group (Figure 8A). Differential genes specific to the low-concentration treatment group were not significantly enriched in the KEGG pathway (Figure 7F). In the CK group, Ribosome, Glycolysis/Gluconeogenesis, and Oxidative phosphorylation were enriched between 9h and 120h, and were primarily associated with electron transport chain and hormone regulation (Figure 7H). We found fewer identical differential genes between the treatment groups and CK (Figure 8B), and *L. brownii* treated with different concentrations of 2,4-DTBP showed different growth patterns. No significant enrichment pathways were found in *L. brownii* subjected to low-concentration 2,4-DTBP treatment. However, GO annotation indicated that differential genes were involved in the response of *L. brownii* to acid, organic nitrogen

compounds, and endogenous stimuli throughout the low-concentration treatment. High concentrations of 2,4-DTBP had a regulatory effect on the phytohormone and MAPK signaling pathways in *L. brownii*. Secondary metabolic pathways such as phenylpropane, flavonoids and Stilbenoid, diarylheptanoid, and gingerol biosynthesis were actively involved in the response to 2,4-DTBP.

3.6 2,4-DTBP got an impact on the oxidative phosphorylation and hormones of *L.brownii*

There was no significant difference observed in appearance between the control group and the treatment group after the first nine hours in touching with 2,4-DTBP (Figures 9A-F). The SDH activity was upregulated in the low concentration group with a short exposure (9h) to 2,4-DTBP compared to the control group (Figure 9K), and was significantly higher than that observed in the high concentration group. Leaf of the treatment group massive withered after 120 hours (Figures 9H-J), the SDH activity are decreased in two treatment groups than the control group. SDH

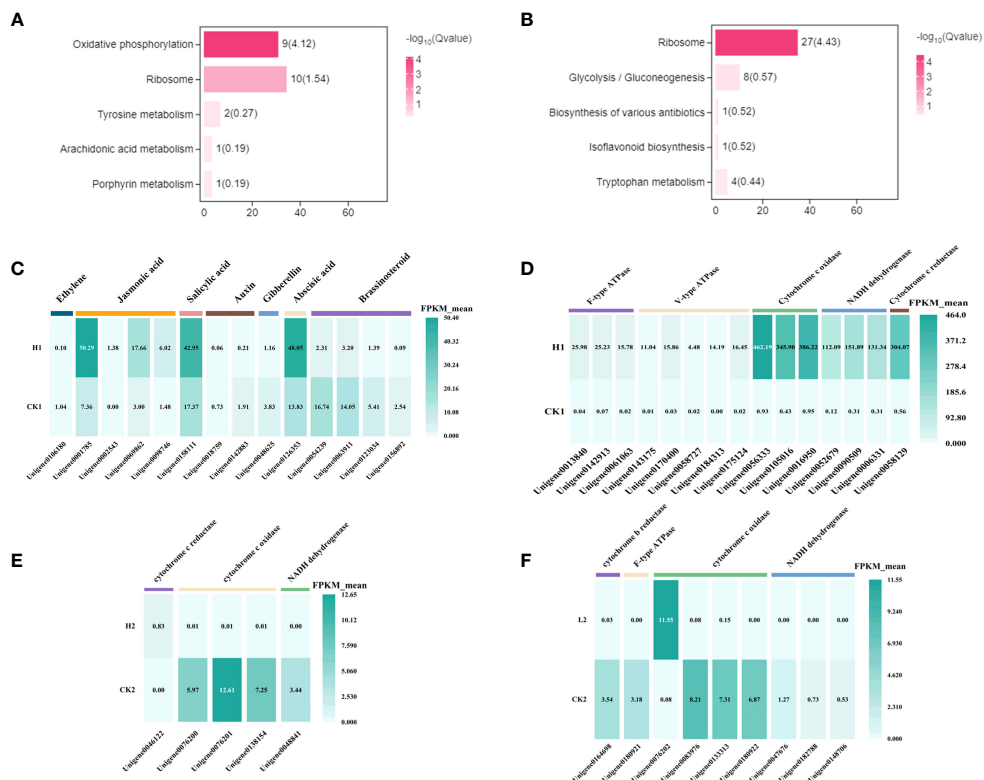


FIGURE 6 The enriched KEGG pathways of the DEGs. Choosing DEGs was only specifically present in various periods of the low-concentration treatment group. **(A)** 9h **(B)** 24h. The vertical axis describes the name of the pathway, and the horizontal axis shows the number of genes in the pathway. **(C)** Heatmap representing expression dynamics of genes involved in phytohormones at 9h CK vs H. group. **(D)** Heatmap representing expression dynamics of genes involved in Oxidative phosphorylation at 9h CK vs H. group. Heatmap representing expression dynamics of genes involved in Oxidative phosphorylation at 24h **(E)** CK vs H. and **(F)** CK vs L. group.

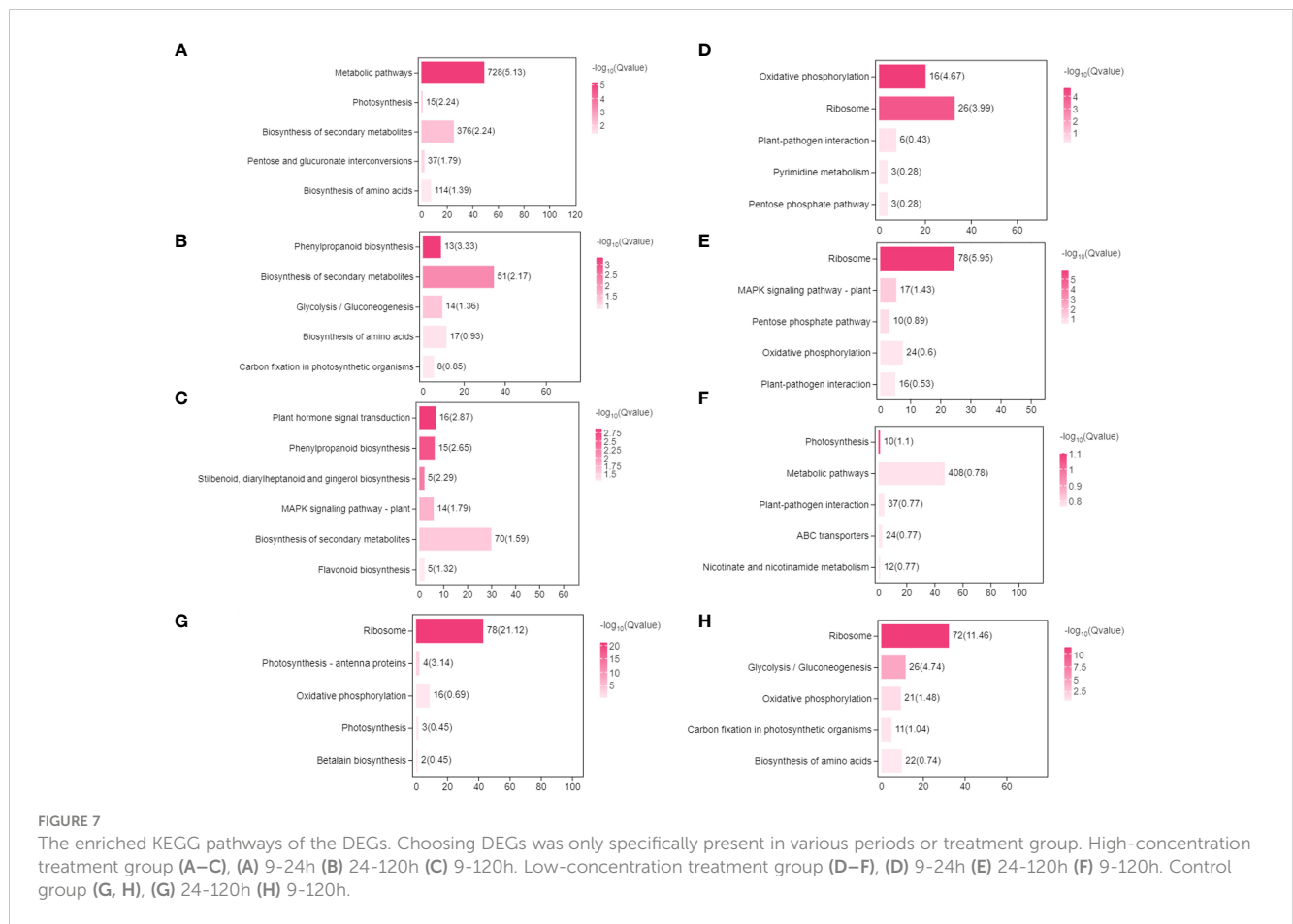
activity of high concentration group remained suppressed throughout the experiment. DEGs in **Figures 6C, D** pertinent with oxidative phosphorylation and hormones pathways were selected for qPCR (**Figure 9L**), the results are the same as the transcriptome.

4 Discussion

Previous studies identified 2,4-DTBP as an autotoxic substance in *Lilium davidii* Duch. ex Elwes (Cui et al., 2022) and *Atractylodes macrocephala* Koidz (Zheng, 2018). Cui et al. (2022) found the rhizosphere of *Lilium davidii* exhibited reduced soil enzyme activity and a suppressed microbial community, and that 2 mmol/L of 2,4-DTBP increased the level of pathogenic fungi such as *Fusarium*. Recently, 2,4-DTBP has been frequently used as a weed control agent due to its broad-spectrum toxicity to plants (Chuah et al., 2015; Zain et al., 2021). A concentration of 0.8 g/L 2,4-DTBP had a higher inhibitory effect on root and stem length development and significantly inhibited germination of *Allium ascalonicum*.

2,4-DTBP is a phenol that affects the dynamic equilibrium of ROS in plant roots. Low concentrations of phenolic acids increase

plant stress resistance (Mei et al., 2020; Chen et al., 2021; Migut et al., 2021). The accumulation of phenolic acids in the soil leads to soil acidification, where the cells of plant roots are the first to be affected. When phenolic acids enter cells with a higher pH, they dissociate to produce large amounts of hydrogen ions, resulting in a decrease in intracellular pH and depolarization of the intra-membrane environment. Intracellularly, phenolic acid autotoxic substances inhibit the activity of antioxidant enzymes, such as peroxidase (POD) and catalase (CAT), leading to an increase in ROS and lipid peroxidation (Zhang et al., 2018; Wang et al., 2019; Xiao et al., 2019; Marchiosi et al., 2020). Autotoxic substances caused a significant increase in the root cell ROS content of *Angelica Sinensis* (Xin et al., 2019). The determination of ROS in the root tips of treated seedlings indicated that phenolic acid-induced oxidative damage was an essential factor in the development of autotoxicity. Increasing ferulic acid concentration decreased the growth rate of *Oryza sativa* roots and increased ROS, calcium content, and lipoxygenase activity (Chi et al., 2013). Treatment with a low concentration of 2,4-DTBP inhibited POD and SOD in *L. brownii*, resulting in lipid peroxidation and an increase in MDA content. During high-concentration treatment, *L. brownii* may be affected by a combination of abiotic stresses such as osmotic stress,



oxidative stress, and ionic stress. There was no significant difference between POD and SOD activity and CK for any of the time periods except 72h POD activity, which was significantly lower than CK.

Plant growth and development requires ATP which is produced by mitochondrial respiration. Complexes I-IV known as NADH ubiquinone oxidoreductase, succinate dehydrogenase, cytochrome *bc1* complex and Cytochrome *c* oxidase are responsible for the formation of the respiratory chain. Simultaneously, complex V is involved in electron transfer and the establishment of the electrochemical proton gradient across the inner mitochondrial membrane. The Results show that the SDH activity was decreased by long-term exposure to the medium containing the 2,4-DTBP. SDH related to regulates downstream defense and stress gene expression by being the source of mH_2O_2 , and the defective SDH affecting mitochondrial electron activity (Gleason et al., 2011). Under Abiotic stress, ATP is consumed more as a fade-back mechanism. For example, ATP is used in large quantities to scavenge ROS and enhance the antioxidant capacity of plants under stress (Zhu et al., 2022). Excess reactive oxygen radicals disrupt the plant cell membrane structure and oxidize sulfhydryl groups of mitochondrial MPTP-associated proteins to disulfides, promoting MPTP opening. They also cause mitochondrial membrane peroxidation, which results in reduced membrane

fluidity. The phenolic acid produced by continuous cropping causes an excessive accumulation of intracellular ROS by inhibiting the activity of enzymes such as SOD, POD, and CAT (Wang et al., 2019). Oxidative stress affects protein synthesis, and oxidants affect tRNA's post-translational modification ability and stability (Shcherbik and Pestov, 2019). Wurtmann and Wolin (2009) found that oxidized RNA slows down protein synthesis, resulting in the production of aggregated and truncated peptides (Wurtmann and Wolin, 2009).

We isolated and screened the roots, stems, leaves, and bulbs of *Lilium brownii* and identified 2,4-DTBP as an autotoxic substance. The toxicity and enzymatic activity assay results of *L. brownii* following 2,4-DTBP treatment were used to screen three 2,4-DTBP concentrations and three time-point samplings for transcriptome sequencing.

Using the transcriptome data, we conducted a preliminary analysis of the effects of autotoxic substances on *L. brownii*. Different concentrations of 2,4-DTBP had varying effects on the growth and development of *L. brownii*. A response to external autotoxic effects was signaled by regulation of the MAPK-signaling and plant hormone signaling pathways, while secondary metabolic pathways, such as photosynthesis and phenylpropane synthesis and metabolism, were involved as downstream pathways for signaling

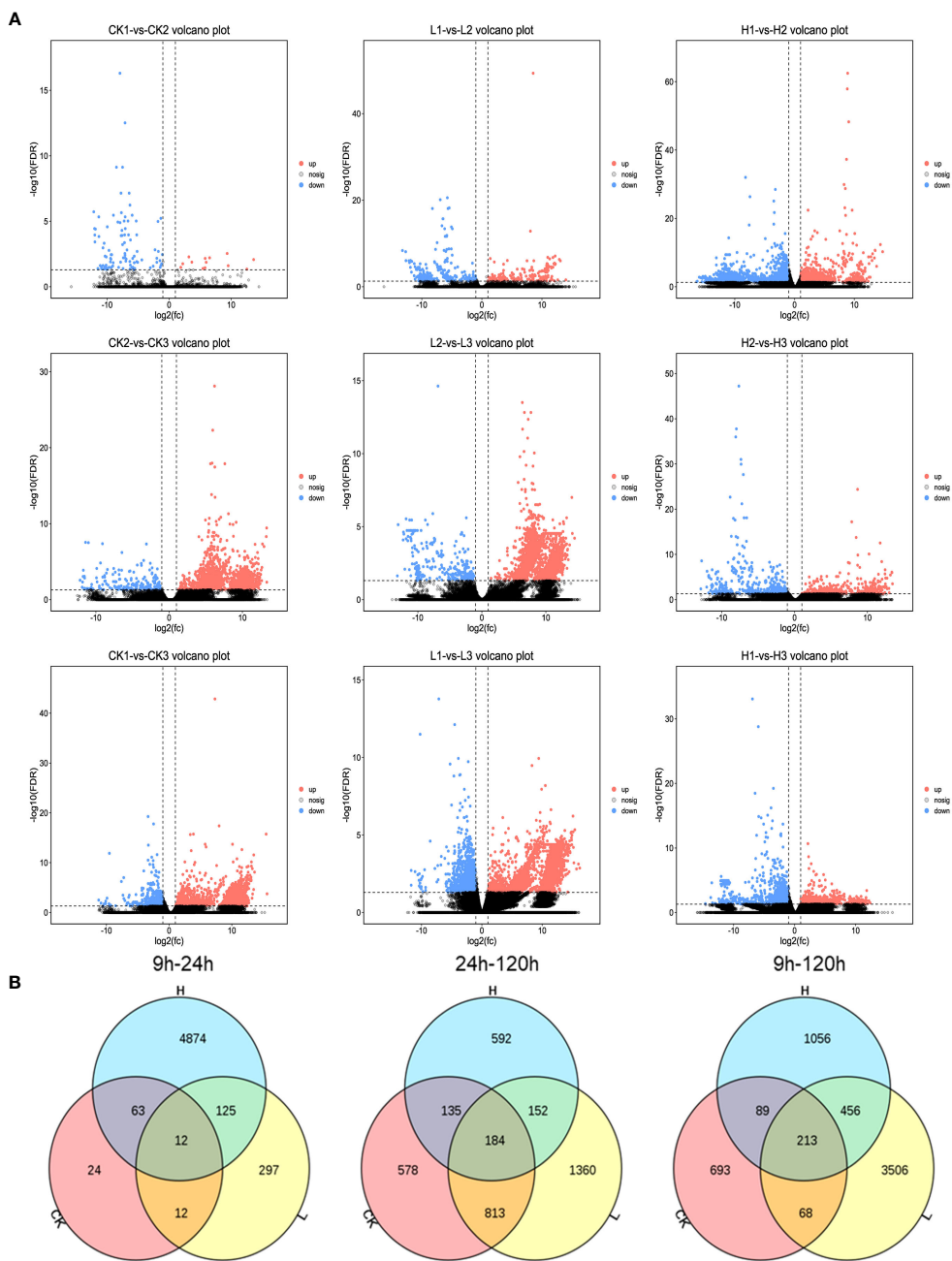


FIGURE 8
(A) Comparison of volcano plots with different periods at the same concentration. The number of DEGs in each tissue is presented and based on the significance shown in the volcano plots. The vertical dash lines in the volcano plots depict the two-fold differential expression cut-off (axis expressed as log₂ values) and the horizontal dash lines shows the -log₁₀(P-value). Dots in red (group₂ up-regulated relative to group₁) and blue (down-regulated) indicate differences in gene expression (FDR < 0.05), while black dots show no differences. **(B)** Venn diagram of DEGs between various treatments.

responses to autotoxic substances. Our findings demonstrate hormonal changes at the transcriptional level in *L. brownii*. Endogenous plant hormones are affected by phenolic compounds (Desmedt et al., 2021). Following 2,4-DTBP treatment for 9h, the expression of phytohormone-related genes was upregulated in *L. brownii*. High BPA concentrations in soybean roots can inhibit root growth at the seedling stage by reducing the content of IAA, ZT, GA3, and ETH in roots and increasing the content of ABA (Li et al., 2018).

This has also been observed in Arabidopsis (Bahmani et al., 2020). Hormones play a role in the response of plants to abiotic stresses (Zhou et al., 2018; Peng et al., 2021). For example, SA is related to the dynamic balance of plant ROS (La et al., 2019; Poór, 2020), and salt stress alters the content of plant hormones such as ABA and IAA (Wu et al., 2017). Additionally, ABA-promoted ROS in the mitochondria of Arabidopsis root tips is an essential retrograde signal that regulates root meristem activity by controlling auxin

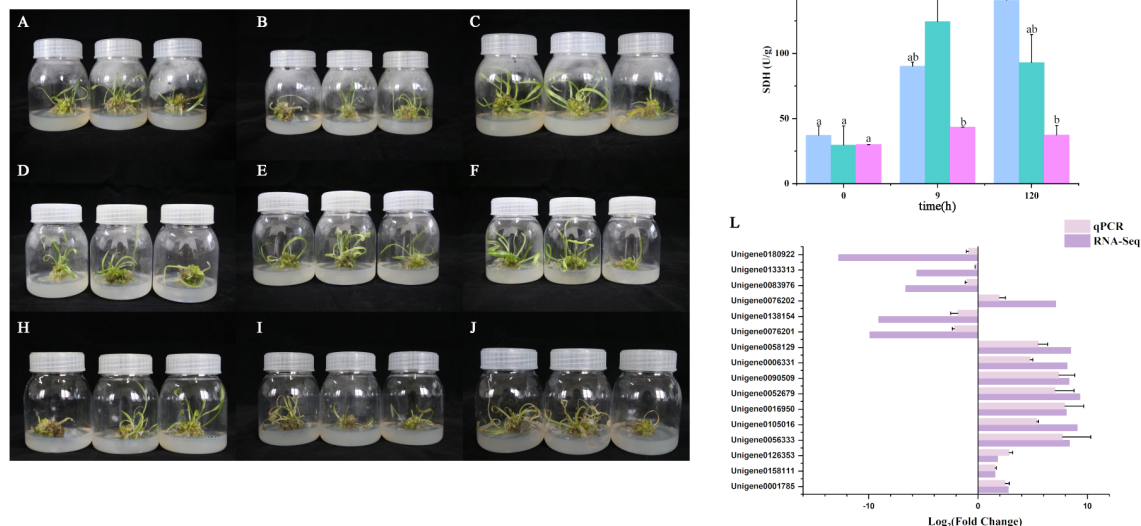


FIGURE 9 Tissue culture seedlings with consistent growth of *L. brownii* which treatment with 0 (A–C), 0.2 (D–F) and 0.8 (H–J) g/L of 2,4-DTBP for 0, 9 and 120 hours. (K) The succinate dehydrogenase (SDH) activity of *L. brownii*. Values represent the mean + SEM (n=3). (L) QPCR result of DEGs in Figures 6C, D pertinent with oxidative phosphorylation and hormones pathways.

accumulation/signaling and PLT expression (Yang et al., 2014). Further studies are required to determine the specific changes in plant hormone content in response to autotoxic substances.

Plant hormone signaling, ROS, and the MAPK-signaling pathway are all involved in signaling activation and transmission in response to autotoxic substance stress. However, the mechanisms underlying these three processes needs further investigation. More research is required to confirm the specific effects of autotoxic substances on mitochondria and ribosomes and the role of each pathway in alleviating the onset of autotoxicity in *L. brownii*.

Data availability statement

The datasets presented in this study can be found in online repositories. The names of the repository/repositories and accession number(s) can be found below: Bioproject accession number: PRJNA1056156.

Author contributions

SZ: Conceptualization, Investigation, Writing – original draft, Writing – review & editing. CG: Conceptualization, Investigation, Writing – review & editing. LuS: Resources, Writing – review & editing. HJ: Resources, Writing – review & editing. X-EW: Resources, Writing – review & editing. LiS: Writing – review & editing, Supervision. XGL: Writing – review & editing. XLL: Writing – review & editing, Project administration, Supervision,

Funding acquisition. JX: Project administration, Supervision, Writing – review & editing.

Funding

The author(s) declare that financial support was received for the research, authorship, and/or publication of this article. This work was supported by the National Key Research and Development Program of China [2016YFD0300905-03], Scientific research project of Hunan Provincial Department of Education [20A242], and Natural Science Foundation of Hunan Province of China [2022JJ30300].

Conflict of interest

The authors declare that the research was conducted in the absence of any commercial or financial relationships that could be construed as a potential conflict of interest.

Publisher’s note

All claims expressed in this article are solely those of the authors and do not necessarily represent those of their affiliated organizations, or those of the publisher, the editors and the reviewers. Any product that may be evaluated in this article, or claim that may be made by its manufacturer, is not guaranteed or endorsed by the publisher.

Supplementary material

The Supplementary Material for this article can be found online at: <https://www.frontiersin.org/articles/10.3389/fpls.2024.1330061/full#supplementary-material>

References

- Adamakis, I.-D. S., Malea, P., Sperdouli, I., Panteris, E., Kokkinidi, D., and Moustakas, M. (2021). Evaluation of the spatiotemporal effects of bisphenol A on the leaves of the seagrass *Cymodocea nodosa*. *J. Hazardous Materials* 404, 124001. doi: 10.1016/j.jhazmat.2020.124001
- Ahuja, I., Kissen, R., and Bones, A. M. (2012). Phytoalexins in defense against pathogens. *Trends Plant Sci.* 17, 73–90. doi: 10.1016/j.tplants.2011.11.002
- Bahmani, R., Kim, D., Modareszadeh, M., Thompson, A. J., Park, J. H., Yoo, H. H., et al. (2020). The mechanism of root growth inhibition by the endocrine disruptor bisphenol A (BPA). *Environ. pollut.* 257, 113516. doi: 10.1016/j.envpol.2019.113516
- Chen, P., Wang, Y., Liu, Q., Zhang, Y., Li, X., Li, H., et al. (2020a). Phase changes of continuous cropping obstacles in strawberry (*Fragaria × ananassa* Duch.) production. *Appl. Soil Ecol.* 155, 103626. doi: 10.1016/j.apsoil.2020.103626
- Chen, Y., Huang, L., Liang, X., Dai, P., Zhang, Y., Li, B., et al. (2020b). Enhancement of polyphenolic metabolism as an adaptive response of lettuce (*Lactuca sativa*) roots to aluminum stress. *Environ. pollut.* 261, 114230. doi: 10.1016/j.envpol.2020.114230
- Chen, Y., Yi, N., Yao, S., Zhuang, J., Fu, Z., Ma, J., et al. (2021). CsHCT-mediated lignin synthesis pathway involved in the response of tea plants to biotic and abiotic stresses. *J. Agric. Food Chem.* 69, 10069–10081. doi: 10.1021/acs.jafc.1c02771
- Chi, W.-C., Chen, Y.-A., Hsiung, Y.-C., Fu, S.-F., Chou, C.-H., Trinh, N. N., et al. (2013). Autotoxicity mechanism of *Oryza sativa*: transcriptome response in rice roots exposed to ferulic acid. *BMC Genomics* 14, 351. doi: 10.1186/1471-2164-14-351
- Chuah, T. S., Norhafizah, M. Z., and Ismail, B. S. (2015). Evaluation of the biochemical and physiological activity of the natural compound, 2,4-ditert-butylphenol on weeds. *Crop Pasture Sci.* 66, 214–223. doi: 10.1071/CP13386
- Cui, J., Zhang, E., Zhang, X., Wang, Q., and Liu, Q. (2022). Effects of 2,4-di-tert-butylphenol at different concentrations on soil functionality and microbial community structure in the Lanzhou lily rhizosphere. *Appl. Soil Ecol.* 172, 104367. doi: 10.1016/j.apsoil.2021.104367
- Deng, C., Zhang, X., Zhu, W., and Qian, J. (2004). Gas chromatography-mass spectrometry with solid-phase microextraction method for determination of methyl salicylate and other volatile compounds in leaves of *Lycopersicon esculentum*. *Analytical Bioanalytical Chem.* 378, 518–522. doi: 10.1007/s00216-003-2240-3
- Desmedt, W., Jonckheere, W., Nguyen, V. H., Ameye, M., De Zutter, N., De Kock, K., et al. (2021). The phenylpropanoid pathway inhibitor piperonylic acid induces broad-spectrum pest and disease resistance in plants. *Plant Cell Environ.* 44, 3122–3139. doi: 10.1111/pce.14119
- Erb, M., and Kliebenstein, D. J. (2020). Plant secondary metabolites as defenses, regulators, and primary metabolites: the blurred functional trichotomy. *Plant Physiol.* 184, 39–52. doi: 10.1104/pp.20.00433
- Gallego-Giraldo, L., Posé, S., Pattathil, S., Peralta, A. G., Hahn, M. G., Ayre, B. G., et al. (2018). Elicitors and defense gene induction in plants with altered lignin compositions. *New Phytol.* 219, 1235–1251. doi: 10.1111/nph.15258
- Gao, Z., Han, M., Hu, Y., Li, Z., Liu, C., Wang, X., et al. (2019). Effects of continuous cropping of sweet potato on the fungal community structure in rhizospheric soil. *Front. Microbiol.* 10. doi: 10.3389/fmicb.2019.02269
- Gleason, C., Huang, S., Thatcher, L. F., Foley, R. C., Anderson, C. R., Carroll, A. J., et al. (2011). Mitochondrial complex II has a key role in mitochondrial-derived reactive oxygen species influence on plant stress gene regulation and defense. *Proc. Natl. Acad. Sci. U.S.A.* 108, 10768–10773. doi: 10.1073/pnas.1016060108
- Huang, W., Sun, D., Wang, R., and An, Y. (2021). Integration of transcriptomics and metabolomics reveals the responses of sugar beet to continuous cropping obstacle. *Front. Plant Sci.* 12. doi: 10.3389/fpls.2021.711333
- Kim, D., Kwak, J. I., and An, Y.-J. (2019). Physiological response of crop plants to the endocrine-disrupting chemical nonylphenol in the soil environment. *Environ. pollut.* 251, 573–580. doi: 10.1016/j.envpol.2019.04.101
- Ku, Y., Li, W., Mei, X., Yang, X., Cao, C., Zhang, H., et al. (2022). Biological control of melon continuous cropping obstacles: weakening the negative effects of the vicious cycle in continuous cropping soil. *Microbiol. Spectr.* 10, e01776–e01722. doi: 10.1128/spectrum.01776-22
- La, V. H., Lee, B.-R., Md., T., Park, S.-H., Jung, H., Bae, D.-W., et al. (2019). Characterization of salicylic acid-mediated modulation of the drought stress responses: Reactive oxygen species, proline, and redox state in *Brassica napus*. *Environ. Exp. Bot.* 157, 1–10. doi: 10.1016/j.envexpbot.2018.09.013
- Li, C., Chen, G., Zhang, J., Zhu, P., Bai, X., Hou, Y., et al. (2021). The comprehensive changes in soil properties are continuous cropping obstacles associated with American ginseng (*Panax quinquefolius*) cultivation. *Sci. Rep.* 11, 1–14. doi: 10.1038/s41598-021-84436-x
- Li, X., Li, Y., Ahammed, G. J., Zhang, X.-N., Ying, L., Zhang, L., et al. (2019b). RBOH1-dependent apoplastic H₂O₂ mediates epigallocatechin-3-gallate-induced abiotic stress tolerance in *Solanum lycopersicum* L. *Environ. Exp. Bot.* 161, 357–366. doi: 10.1016/j.envexpbot.2018.11.013
- Li, J., Liu, X., Wang, Q., Huangfu, J., Schuman, M. C., and Lou, Y. (2019a). A group D MAPK protects plants from autotoxicity by suppressing herbivore-induced defense signaling. *Plant Physiol.* 179, 1386–1401. doi: 10.1104/pp.18.01411
- Li, X., Wang, L., Wang, S., Yang, Q., Zhou, Q., and Huang, X. (2018). A preliminary analysis of the effects of bisphenol A on the plant root growth via changes in endogenous plant hormones. *Ecotoxicol. Environ. Saf.* 150, 152–158. doi: 10.1016/j.ecoenv.2017.12.031
- Marchiosi, R., dos Santos, W. D., Constantin, R. P., de Lima, R. B., Soares, A. R., Finger-Teixeira, A., et al. (2020). Biosynthesis and metabolic actions of simple phenolic acids in plants. *Phytochem. Rev.* 19, 865–906. doi: 10.1007/s11101-020-09689-2
- Mei, Y., Sun, H., Du, G., Wang, X., and Lyu, D. (2020). Exogenous chlorogenic acid alleviates oxidative stress in apple leaves by enhancing antioxidant capacity. *Scientia Hort.* 274, 109676. doi: 10.1016/j.scienta.2020.109676
- Migut, D., Janczak-Pieniążek, M., Piechowiak, T., Buczek, J., and Balawejder, M. (2021). Physiological response of maize plants (*Zea mays* L.) to the use of the potassium quercetin derivative. *IJMS* 22, 7384. doi: 10.3390/ijms22147384
- Peng, D., Wang, W., Liu, A., Zhang, Y., Li, X., Wang, G., et al. (2021). Comparative transcriptome combined with transgenic analysis reveal the involvement of salicylic acid pathway in the response of *Nicotiana tabacum* to triclosan stress. *Chemosphere* 270, 129456. doi: 10.1016/j.chemosphere.2020.129456
- Poór, P. (2020). Effects of salicylic acid on the metabolism of mitochondrial reactive oxygen species in plants. *Biomolecules* 10, 341. doi: 10.3390/biom10020341
- Shcherbik, N., and Pestov, D. G. (2019). The impact of oxidative stress on ribosomes: from injury to regulation. *Cells* 8, 1379. doi: 10.3390/cells8111379
- Wang, X. Q., Du, G. D., Lu, X. F., Ma, H. Y., Lyu, D. G., Zhang, H., et al. (2019). Characteristics of mitochondrial membrane functions and antioxidant enzyme activities in strawberry roots under exogenous phenolic acid stress. *Scientia Hort.* 248, 89–97. doi: 10.1016/j.scienta.2018.12.051
- Wang, C., Liu, Z., Wang, Z., Pang, W., Zhang, L., Wen, Z., et al. (2022). Effects of autotoxicity and allelopathy on seed germination and seedling growth in *Medicago truncatula*. *Front. Plant Sci.* 13. doi: 10.3389/fpls.2022.908426
- Wang, X., Wang, J., Zhang, R., Huang, Y., Feng, S., Ma, X., et al. (2018). Allelopathic effects of aqueous leaf extracts from four shrub species on seed germination and initial growth of *amygdalus pedunculata* pall. *Forests* 9, 711. doi: 10.3390/f9110711
- Wu, F., Ding, Y., Nie, Y., Wang, X.-J., An, Y.-Q., Roessner, U., et al. (2021). Plant metabolomics integrated with transcriptomics and rhizospheric bacterial community indicates the mitigation effects of *Klebsiella oxytoca* P620 on p-hydroxybenzoic acid stress in cucumber. *J. Hazardous Materials* 415, 125756. doi: 10.1016/j.jhazmat.2021.125756
- Wu, B., Long, Q., Gao, Y., Wang, Z., Shao, T., Liu, Y., et al. (2015). Comprehensive characterization of a time-course transcriptional response induced by autotoxins in *Panax ginseng* using RNA-Seq. *BMC Genomics* 16, 1010. doi: 10.1186/s12864-015-2151-7
- Wu, X., Riaz, M., Yan, L., Zhang, Z., and Jiang, C. (2020). How the cells were injured and the secondary metabolites in the shikimate pathway were changed by boron deficiency in trifoliolate orange root. *Plant Physiol. Biochem.* 151, 630–639. doi: 10.1016/j.plaphy.2020.04.009
- Wu, W., Zhang, Q., Ervin, E. H., Yang, Z., and Zhang, X. (2017). Physiological mechanism of enhancing salt stress tolerance of perennial ryegrass by 24-epibrassinolide. *Front. Plant Sci.* 8. doi: 10.3389/fpls.2017.01017
- Wurtmann, E. J., and Wolin, S. L. (2009). RNA under attack: Cellular handling of RNA damage. *Crit. Rev. Biochem. Mol. Biol.* 44, 34–49. doi: 10.1080/10409230802594043
- Xiang, W., Chen, J., Zhang, F., Huang, R., and Li, L. (2022). Autotoxicity in *Panax notoginseng* of root exudates and their allelochemicals. *Front. Plant Sci.* 13. doi: 10.3389/fpls.2022.1020626

SUPPLEMENTARY TABLE 1

The list of the identified components in 4 tissues of *Lilium brownii*.

SUPPLEMENTARY TABLE 2

Quality statistics of Longya lily transcriptome sequencing.

SUPPLEMENTARY TABLE 3

9h–24h differential gene GO enrichment analysis (p. adjust < 0.05).

- Xiao, C., Wang, L., Hu, D., Zhou, Q., and Huang, X. (2019). Effects of exogenous bisphenol A on the function of mitochondria in root cells of soybean (*Glycine max* L.) seedlings. *Chemosphere* 222, 619–627. doi: 10.1016/j.chemosphere.2019.01.195
- Xin, A., Li, X., Jin, H., Yang, X., Zhao, R., Liu, J., et al. (2019). The accumulation of reactive oxygen species in root tips caused by autotoxic allelochemicals – A significant factor for replant problem of *Angelica sinensis* (Oliv.) Diels. *Ind. Crops Products* 138, 111432. doi: 10.1016/j.indcrop.2019.05.081
- Yan, W., Cao, S., Wu, Y., Ye, Z., Zhang, C., Yao, G., et al. (2022). Integrated Analysis of Physiological, mRNA Sequencing, and miRNA Sequencing Data Reveals a Specific Mechanism for the Response to Continuous Cropping Obstacles in *Pogostemon cablin* Roots. *Front. Plant Sci.* 13. doi: 10.3389/fpls.2022.853110
- Yang, M., Fan, Z., Xie, Y., Fang, L., Wang, X., Yuan, Y., et al. (2020). Transcriptome analysis of the effect of bisphenol A exposure on the growth, photosynthetic activity and risk of microcystin-LR release by *Microcystis aeruginosa*. *J. Hazardous Materials* 397, 122746. doi: 10.1016/j.jhazmat.2020.122746
- Yang, L., Zhang, J., He, J., Qin, Y., Hua, D., Duan, Y., et al. (2014). ABA-mediated ROS in mitochondria regulate root meristem activity by controlling PLETHORA expression in *Arabidopsis*. *PLoS Genet.* 10, e1004791. doi: 10.1371/journal.pgen.1004791
- Yu, B., Pan, Y., Liu, Y., Chen, Q., Guo, X., and Tang, Z. (2021). A comprehensive analysis of transcriptome and phenolic compound profiles suggests the role of flavonoids in cotyledon greening in *Catharanthus roseus* seedling. *Plant Physiol. Bioch* 167, 185–197. doi: 10.1016/j.plaphy.2021.07.028
- Zain, N. M., Che, M. M., and Tse, S. C. (2021). Pre-emergence herbicidal activity and persistence of 2,4-di-tertbutylphenol in relation to soil types. *Plant Omics* 14, 30–37. doi: 10.21475/poj
- Zeng, J., Liu, J., Lu, C., Ou, X., Luo, K., Li, C., et al. (2020). Intercropping with turmeric or ginger reduce the continuous cropping obstacles that affect *Pogostemon cablin* (Patchouli). *Front. Microbiol.* 11, 579719. doi: 10.3389/fmicb.2020.579719
- Zhang, J., Wang, L., Zhou, Q., and Huang, X. (2018). Reactive oxygen species initiate a protective response in plant roots to stress induced by environmental bisphenol A. *Ecotoxicol Environ. Saf.* 154, 197–205. doi: 10.1016/j.ecoenv.2018.02.020
- Zhang, Z., Zhang, Z., Han, X., Wu, J., Zhang, L., Wang, J., et al. (2020). Specific response mechanism to autotoxicity in melon (*Cucumis melo* L.) root revealed by physiological analyses combined with transcriptome profiling. *Ecotoxicol Environ. Saf.* 200, 110779. doi: 10.1016/j.ecoenv.2020.110779
- Zheng, F. (2018). Identification of autotoxic compounds from *Atractylodes macrocephala* Koidz and preliminary investigations of their influences on immune system. *J. Plant Physiol.* 230, 33–39. doi: 10.1016/j.jplph.2018.08.006
- Zhou, Y., Huo, S., Wang, L., Meng, J., Zhang, Z., and Xi, Z. (2018). Exogenous 24-Epibrassinolide alleviates oxidative damage from copper stress in grape (*Vitis vinifera* L.) cuttings. *Plant Physiol. Biochem.* 130, 555–565. doi: 10.1016/j.plaphy.2018.07.029
- Zhu, A., Li, J., Fu, W., Wang, W., Tao, L., Fu, G., et al. (2022). Abscisic acid improves rice thermo-tolerance by affecting trehalose metabolism. *Int. J. Mol. Sci.* 23, 10615. doi: 10.3390/ijms231810615